Check for updates

esa

ECOSPHERE

COASTAL AND MARINE ECOLOGY

Patterns of depredation in the Hawai'i deep-set longline fishery informed by fishery and false killer whale behavior

Joseph E. Fader,[1,†] Robin W. Baird,[2] Amanda L. Bradford,[3] Daniel C. Dunn,[4] Karin A. Forney,[5,6] and Andrew J. Read[1]

[1]*Division of Marine Science and Conservation, Nicholas School of the Environment, Duke University Marine Lab, Beaufort, North Carolina 28516 USA*
[2]*Cascadia Research Collective, Olympia, Washington 98501 USA*
[3]*Pacific Islands Fisheries Science Center, NOAA Fisheries, Honolulu, Hawaii 96818 USA*
[4]*School of Earth and Environmental Sciences, University of Queensland, Brisbane, Queensland 4072 Australia*
[5]*Marine Mammal and Turtle Division, Southwest Fisheries Science Center, National Marine Fisheries Service, National Oceanic and Atmospheric Administration, Moss Landing, California, USA*
[6]*Moss Landing Marine Laboratories, San Jose State University, Moss Landing, California, USA*

Citation: Fader, J. E., R. W. Baird, A. L. Bradford, D. C. Dunn, K. A. Forney, and A. J. Read. 2021. Patterns of depredation in the Hawai'i deep-set longline fishery informed by fishery and false killer whale behavior. Ecosphere 12(8):e03682. 10.1002/ecs2.3682

Abstract. False killer whales (*Pseudorca crassidens*) depredate bait and catch in the Hawai'i-based deep-set longline fishery, and as a result, this species is hooked or entangled more than any other cetacean in this fishery. We analyzed data collected by fisheries observers and from satellite-linked transmitters deployed on false killer whales to identify patterns of odontocete depredation that could help fishermen avoid overlap with whales. Odontocete depredation was observed on ~6% of deep-set hauls across the fleet from 2004 to 2018. Model outcomes from binomial GAMMs suggested coarse patterns, for example, higher rates of depredation in winter, at lower latitudes, and with higher fishing effort. However, explanatory power was low, and no covariates were identified that could be used in a predictive context. The best indicator of depredation was the occurrence of depredation on a previous set of the same vessel. We identified spatiotemporal scales of this repeat depredation to provide guidance to fishermen on how far to move or how long to wait to reduce the probability of repeated interactions. The risk of depredation decreased with both space and time from a previous occurrence, with the greatest benefits achieved by moving ~400 km or waiting ~9 d, which reduced the occurrence of depredation from 18% to 9% (a 50% reduction). Fishermen moved a median 46 km and waited 4.7 h following an observed depredation interaction, which our analysis suggests is unlikely to lead to large reductions in risk. Satellite-tagged pelagic false killer whales moved up to 75 km in 4 h and 335 km in 24 h, suggesting that they can likely keep pace with longline vessels for at least four hours and likely longer. We recommend fishermen avoid areas of known depredation or bycatch by moving as far and as quickly as practical, especially within a day or two of the depredation or bycatch event. We also encourage captains to communicate depredation and bycatch occurrence to enable other vessels to similarly avoid high-risk areas.

Key words: bycatch; cetacean; depredation; false killer whale; odontocete; pelagic longline fishery.

Received 30 November 2020; revised 23 March 2021; accepted 30 March 2021. Corresponding Editor: Hunter S. Lenihan.
Copyright: © 2021 The Authors. This is an open access article under the terms of the Creative Commons Attribution License, which permits use, distribution and reproduction in any medium, provided the original work is properly cited.
† **E-mail:** joefader@gmail.com

Introduction

Many marine predators engage in depredation by consuming bait or fish secured on fishing gear. This behavior is very common and costly in longline fisheries worldwide (Read 2008, Hamer et al. 2012). Odontocetes, or toothed whales, are particularly adept at depredation and can remove large quantities of catch, often with substantial economic impacts (Tixier et al. 2020). Depredation reflects a switch from natural foraging behavior of prey pursuit to feeding on often high-energy but restrained prey. This behavior may reduce the energetic costs of foraging but increases the risk of hooking or entanglement in fishing gear. False killer whales (*Pseudorca crassidens*) depredate catch in a number of pelagic longline fisheries worldwide, including the Hawai'i-based, deep-set longline fishery that targets bigeye tuna (*Thunnus obesus*; Forney et al. 2011). False killer whales are the most frequently bycaught cetacean in this fleet, and estimated fishery-related mortality and serious injury of this species has repeatedly exceeded allowable levels under the U.S. Marine Mammal Protection Act (MMPA; Carretta et al. 2009). In the present study, we examine patterns of odontocete depredation in the Hawai'i deep-set fishery and the behavior of tagged false killer whales to identify predictive factors that could be used to potentially reduce harmful interactions and the cost of depredation to fishermen.

At a global scale, depredation and subsequent marine mammal bycatch in longline fisheries has been an exceedingly difficult problem to solve, despite consideration of a wide range of mitigation strategies (e.g., Werner et al. 2015). The incentives to feed on large, energetically dense captured fish are likely high (Esteban et al. 2016), making it very difficult to create disincentives to this behavior. In addition, interactions are seldom observed directly, as they often occur at depth, at night, or far from the vessel (Werner et al. 2015). Acoustic harassment devices have been considered as a means of deterring marine mammals from engaging in depredation and reducing bycatch (Werner et al. 2015, Hamilton and Baker 2019), although in the case of longline depredation, odontocetes may habituate quickly to these signals and even be attracted to deterrents that notify whales of the location of catch, an apparent dinner bell effect (Mooney et al. 2009, Tixier et al. 2015*a*). Many strategies thus focus on technological innovations that limit impacts after animals have encountered fishing gear. Gear modifications such as physical devices designed to protect catch (Rabearisoa et al. 2012) or weak hooks, designed to release hooked cetaceans, are in use in some fisheries (Bayse and Kerstetter 2010, Bigelow et al. 2012), including the Hawai'i deep-set fishery (weak hooks). However, these approaches can be costly and unwieldy to deploy (catch protection) or ineffective in reducing the incidence of depredation (weak hooks).

An alternative strategy is to adjust fishing behavior or operations to allow fishermen to avoid interactions with depredating species in the first place (e.g., Stepanuk et al. 2018, Tixier et al. 2019). Such an approach might be implemented at two spatial scales: (1) predicting interactions a priori from broad-scale environmental drivers of overlap between fisheries and bycatch and (2) understanding fine-scale behavior of depredators around gear to avoid interactions despite whale co-occurrence. Many pelagic predators range widely and their patterns of distribution may be influenced by static (e.g., seafloor topography; Lindsay et al. 2016, Thorne et al. 2017) or dynamic oceanographic features (e.g., sea surface temperature [SST] fronts; Howell et al. 2008, Woodworth et al. 2011, Hazen et al. 2017). Pelagic fishing vessels also range widely, tracking specific oceanographic conditions, and when the distribution of fishing activities converges with the distribution of depredating species in space and time, interactions may occur (Howell et al. 2008, Thorne et al. 2017, 2019, Stepanuk et al. 2018). Identifying the ecological drivers of this co-occurrence could help fishermen avoid overlap and subsequent interactions.

Given broad-scale spatiotemporal co-occurrence, depredation is further driven by the depredator's behavior in the vicinity of fishing gear. The cues that depredating animals use to locate gear and their behavior during and around fishing operations are often species- and fishery-specific and thus are important to understand when developing mitigation strategies,

such as limiting depredator access to gear or avoiding acoustic detection by depredators. For example, demersal longline fishing involves setting gear directly on the seafloor, and due to the extreme depths that this gear is fished (500–2000 m), depredation interactions are thought to occur mostly during the hauling phase (but see Richard et al. 2020, 2021). In contrast, pelagic longline gear is suspended in the water column closer to the surface, and thus, the gear is potentially accessible to depredation for the full duration of a fishing event (Rabearisoa et al. 2012, Thode et al. 2016). Acoustic signatures from vessels or gear are likely important cues for depredating odontocetes in both fishery types, although there are surely nuances in each case. Sperm whales (*Physeter macrocephalus*) depredating demersal longlines in southeast Alaska appear to respond to very specific acoustic signatures from the cavitation of a ship's propeller when the engine is engaged to haul gear, detecting these sounds from several kilometers and arriving at a haul within minutes of a vessel beginning to retrieve gear (Thode et al. 2007, 2015). Passive acoustic monitoring of pelagic longline gear deployments detected false killer whales most commonly during the hauling phase, with whales moving along the mainline away from the vessel as gear was being retrieved (Bayless et al. 2017). Anderson et al. (2020) observed satellite-tagged false killer whales orienting their movements toward pelagic longline gear most commonly during the hauling phase, although they did not do so every time they were within likely detection range.

False killer whale depredation and bycatch

False killer whales are social, highly mobile, apex predators that occur in tropical and subtropical oceans worldwide. Independently of fisheries, they are known to feed on a range of pelagic fish species, including tunas (*Thunnus* spp.), mahi-mahi (*Coryphaenus hippurus*), and wahoo (*Acanthocybium solandri*; Baird et al. 2008), all of which are commonly captured in the Hawai'i deep-set longline fishery. Three partially overlapping populations of false killer whales are recognized around the Hawaiian Islands: an endangered, insular population around the main Hawaiian Islands (MHIs; Baird et al. 2008, Bradford et al. 2018); an insular population closely associated with the Northwestern Hawaiian Islands (NWHIs; Baird et al. 2013); and a pelagic population that ranges broadly within and beyond the U.S. exclusive economic zone (EEZ; Bradford et al. 2015, Anderson et al. 2020). Most false killer whale bycatch in the Hawai'i longline fleet involves the pelagic population, as vessels are restricted from fishing within the core range of the MHI population and are not permitted to fish in the Papahānaumokuākea Marine National Monument, which includes waters surrounding the NWHIs.

There are two distinct Hawai'i-based, pelagic longline fisheries. Most effort occurs in the deep-set fishery, which targets bigeye tuna and operates year-round to the north and south of the Hawaiian Islands, both inside and outside of the U.S. EEZ. A smaller, shallow-set fishery targets swordfish (*Xiphias gladius*), operating mainly north of the Hawaiian Islands. Hawai'i longline captains must fish with the same gear configuration (deep or shallow) for the duration of a trip. Regulations have been adopted to reduce the bycatch of several protected species in both fisheries. High rates of sea turtle bycatch led to the closure of shallow-set operations in 2003–2004 (Gilman et al. 2007), and both fisheries have enacted operational and gear changes to mitigate sea turtle and seabird bycatch (Gilman et al. 2007, 2008), primarily in response to litigation. Odontocete depredation and bycatch is a more common problem for the deep-set fishery (Forney et al. 2011), which is the focus of the current study. As in other pelagic longline fisheries experiencing odontocete depredation (e.g., Secchi and Vaske 1998, Rabearisoa et al. 2018), depredation by toothed whales is rarely observed directly in the deep-set fishery (Bayless et al. 2017), but rather inferred by characteristic damage to individual caught fish retrieved during the haul (Forney et al. 2011).

A variety of odontocete species have been observed as bycatch in this fishery, including false killer whales, short-finned pilot whales (*Globicephala macrorhynchus*), and Risso's dolphins (*Grampus griseus*; Forney and Kobayashi 2007). High levels of false killer whale bycatch led to formation of the False Killer Whale Take Reduction Team (TRT) in 2010, a multi-stakeholder group charged with reducing mortality and serious injury of false killer whales below levels stipulated

by the MMPA. The U.S. National Marine Fisheries Service (NMFS) published a final Take Reduction Plan in 2012 (77 FR 71260) (Federal Register 2012). The primary regulatory tool for mitigating bycatch was a requirement for vessels to use a combination of weak circle hooks (specified by a maximum shank diameter of 4.5 mm) and strong terminal gear (minimum 2.0 mm branch line diameter) to allow release of hooked false killer whales while retaining target catch. Recently, the team has acknowledged that these measures are not significantly reducing serious injury or mortality of false killer whales and have recommended studies to investigate the possibility of a transition to even weaker hooks (i.e., narrower diameter) and stronger (i.e., thicker diameter) branch lines (False Killer Whale Take Reduction—Key outcomes memoranda and summaries. Accessed on 14 September 2020 at https://www.fisheries.noaa.gov/national/marine-mammal-protection/false-killer-whale-take-reduction). This approach is designed to maximize the likelihood of survival for animals that become hooked, but it does not reduce the economic cost of depredation to the fishery.

Avoiding interactions outright would benefit both whales and fishermen, and there has been long-standing interest from the false killer whale TRT to identify patterns and proximate mechanisms driving depredation. To this end, Forney et al. (2011) conducted a multivariate analysis of false killer whale depredation and bycatch between 2003 and 2009 to assess the influence of environmental and operational covariates on the occurrence of interactions. The analysis identified few clear environmental covariates of depredation and bycatch, except for a seasonal pattern of lower depredation in summer when the fleet fishes farther to the north, likely beyond the primarily tropical and subtropical range of pelagic false killer whales. The authors found evidence that sets were more likely to experience odontocete depredation if the preceding set was depredated and that moving 100 km following depredation led to a slight (~16%) decrease in the risk of subsequent depredation. These findings suggest either pursuit of fishing vessels by depredators or clumping of whales in space and time, although at the time there were insufficient data to assess patterns in space and time simultaneously.

This previous work has provided important insights into the processes driving false killer whale depredation, but this behavior remains poorly understood and unmitigated. Here, we incorporate nine years of additional fisheries observer data to expand the analysis of Forney et al. (2011). This larger dataset provides more power to explore environmental and operational covariates and the ability to examine patterns in repeat depredation in both space and time across the fleet. We also analyze typical speeds and distances traveled by satellite-tagged pelagic false killer whales, allowing comparison of depredator movement behavior to the spatiotemporal patterns of depredation observed from fishery-dependent data. An improved understanding of broad- and fine-scale patterns of depredation, and the animal behavior driving these interactions, will help inform efforts to reduce the negative consequences of depredation and bycatch for both whales and fishermen.

Methods

Study area and fishery-dependent data sources

Hawai'i deep-set gear consists of a single monofilament mainline (3.2–4.0 mm diameter) suspended in the water column by a series of floats (Appendix S1: Fig. S1). Individual branch lines with a mackerel-type bait on a single hook are regularly spaced along ~45–80 km of mainline (Boggs and Ito 1993). The target depth for bigeye tuna is around 400 m and a typical deployment of fishing gear ranges from 1000 to 3000 hooks. Deep-set fishermen generally deploy (set), their gear in the morning, allowing it to fish (soak) until the retrieval (haul), begins around sundown. The hauling process may exceed 12 h, depending on the catch and amount of gear deployed. We describe the full process of a single fishing event (i.e., the start of a set to the end of the haul) as a single deployment or event, unless referring to a more specific step of the process.

Fishery-dependent data were derived from two sources: logbook data recorded by vessel captains and data collected by fisheries observers. For each deployment, captains are required to record and submit to NMFS the times and GPS coordinates of the start and finish of setting and hauling of gear (i.e., four times and locations per fishing event), the number of hooks

deployed, and counts of caught fish by species. By regulation, deep-set vessels are required to carry a federal observer, if requested, with a fleet-wide target coverage of 20% of all trips. Observers collect more detailed data on fishing effort, gear characteristics, and biological data from both target and non-target catch, including bycatch of protected species. Since late 2003, observers have also been trained to classify and systematically record depredation (i.e., damage to catch). Of interest in this study is odontocete depredation, which can be distinguished from other sources of depredation, such as squid or sharks, because toothed whales often predate the whole fish up to the gill plates, leaving only the head attached to the hook (e.g., Secchi and Vaske 1998). False killer whales are also known to depredate bait (Thode et al. 2016), but this is not systematically recorded by observers and is thus not reported here. Based on covariate data availability and model formulations, the multivariate analyses of depredation described below utilize observer-collected data from 2004 to 2017, while the spatial analyses utilize observer data from 2004 to 2018.

Derivation of covariates

We identified spatial, temporal, gear, operational, and environmental variables hypothesized to influence odontocete depredation rate (Appendix S1: Table S1). Space and time variables were associated with the start of the haul of the focal fishing deployment, as recorded by the onboard observer. Gear and operational variables were also based on observer-reported values for each fishing event, with the exception of vessel density, which utilized logbook data to calculate the number of all (i.e., not just observed) vessels that began a haul within 200 km and ±3 d of the observed (focal) haul. Number of hooks represents the total number of individual hooks deployed in the focal fishing event. Soak was calculated as the time (h) between the last piece of gear entering the water (end of set) to the last piece of gear removed from the water (end of haul). Minimum depth of gear (m) is the sum of all vertical pieces of gear (float line + branch line + leader), but due to shoaling and concatenation of the mainline, actual depth of gear varies widely throughout the soak and haul (Bigelow et al. 2006). Hooks between floats was used as a secondary indicator of gear depth, as more hooks between floats generally means the gear sinks deeper. All catch and catch per unit effort (CPUE) variables were derived from observer-recorded counts of hooked (not necessarily landed or kept) target and non-target catch. CPUE (number of fish caught per 1000 hooks) was based on all hooked bony fish (i.e., not including sharks) in a haul. As an indicator of catch on nearby vessels, we also calculated the CPUE of tuna species (number of tunas caught per 1000 hooks) caught on observed vessels that began a haul within 100 km and ±1 d of the focal haul. We further identified, for each observed haul, whether odontocete depredation or bycatch of a false killer whale was recorded by the observer during the previous haul of the same vessel, with the first haul of each trip included but treated as an absence of previous depredation.

Environmental variables included both static and dynamic variables and most were associated with haul-begin location, with any distances calculated as the great circle distance (km) from the haul-begin location to the feature. We acknowledge that haul-begin location is only an approximate representation of fishing location as longlines can be tens of kilometers long; however, we believe haul-begin location to be a reasonable characterization due to false killer whales evidently orienting most commonly to the hauling phase (Bayless et al. 2017, Anderson et al. 2020). The static variable depth and slope were derived from GEBCO 30 arc-second bathymetry data; and distance to nearest seamount was derived from the seamount database described in Allain et al. (2008)

Sea surface temperature (SST) range was calculated as the difference between the highest and lowest SST (°C) for all four recorded fishing locations per deployment, with SST derived from Level 4 daily, nighttime interpolated SST provided by the Group for High Resolution Sea Surface Temperature (JPL MUR MEaSUREs Project 2015). Chlorophyll-*a* concentration (mg/m^3) was Level 3 monthly, 9 km resolution from the Aqua MODIS satellite (OBPG 2014). Absolute dynamic topography (adt, m), which is a measure of sea surface height, and total kinetic energy (tke, m^2/s^2) were derived from the Archiving, Validation and Interpretation of Satellite Oceanographic

data group hosted by the Copernicus Marine Environment Monitoring Service. Eddy distance and amplitude of the nearest eddy were derived from the database described in Chelton et al. (2011). Distance to oceanographic fronts was the distance to the nearest Cayula-Cornelius thermal front (Cayula and Cornillon 1992). El Niño-Southern Oscillation (ENSO) conditions were considered based on the Oceanic Niño Index (ONI; 3-month running mean of Extended Reconstructed Sea Surface Temperature [v4] anomalies in the Niño 3.4 region; 5° N–5° S, 120°–170° W). We also conducted a lag-correlation analysis between the average monthly rate of odontocete depredation (centered and with seasonal trend removed) and monthly ONI, to assess whether there was a delayed response to ENSO conditions. This identified a peak correlation in depredation 11 months following ONI (Appendix S1: Fig. S2), and thus, we included a variable for the 11-month lag value of ONI in addition to concurrent ONI in models. We used various tools in the Marine Geospatial Ecology Toolbox for extraction of many of the environmental variables (Roberts et al. 2010).

Multivariate data analysis

We conducted a detailed data exploration and analysis to examine the influence of potential predictor variables on the occurrence of odontocete depredation in the deep-set fishery from 2004 to 2017. We first assessed collinearity among explanatory variables by calculating Pearson correlation coefficients for all pairwise combinations of continuous variables, retaining only those with values <0.5. When two variables with similar ecological meaning were correlated, we retained the one with fewer missing values or a clearer ecological relationship to the response. After a first selection, we assessed the variables considered in the full models (Appendix S1: Table S1) using the variance inflation factor (VIF), ensuring that none exceeded a threshold of 3. As the VIF of each variable depends on the other variables present, we recalculated VIF after model selection, ensuring that no correlated variables were retained in the final models either. We also assessed concurvity (Wood 2006) among variables in candidate final models to ensure that no variables were nonlinearly related.

We then used generalized additive mixed models (GAMMs) to examine the relationship between retained variables and the occurrence of odontocete depredation. GAMMs are a regression approach that calculate smooth functions to estimate relationships between predictor and response variables (Wood 2017). We chose GAMMs as we were interested in exploring the combined influence of a range of different variable types in a single model. The GAMM approach allows greater flexibility in specifying different terms within a single model, with fewer a priori assumptions on the nature of each relationship, than, for example, generalized linear models (Wood 2017). A GAMM uses a link function $g()$ to relate a univariate response variable Y to a sum of smooth functions of the covariates X_i:

$$g(E(Y)) = \alpha + \sum f_i(X_i)$$

where α is the intercept and f_i is a smooth function of the covariate X_i.

We used a logit link function to model the relationship between covariates and the binomial presence or absence of odontocete catch damage on at least one fish during a single set. To increase sample size, we also included the occurrence of a hooked or entangled false killer whale as a presence, which added 29 observations. Although other odontocetes likely engage in depredation on Hawai'i deep-set gear, we included only false killer whale bycatch as this species is the most frequently bycaught odontocete, and we wanted the models to be as specific to false killer whales as possible. We explored two possibilities for a fully saturated model, one with no interactions (Appendix S1: Eq. S1) and one including several interactions informed from exploratory analyses and a priori hypotheses (Appendix S1: Eq. S2). These included interactions between month and latitude, month and ONI lag, and latitude and ONI lag. Following Zuur et al. (2009), we began model selection from the fully saturated models with penalized thin-plate regression splines used for all univariate smoothers and tensor product smooths for any interaction terms. We modeled month using a cyclic regression spline to ensure a smooth step from December to January. We treated the presence or absence of depredation on the previous set of the focal vessel as a categorical, parametric

variable and vessel identity as a random effect to control for variation within vessels and individual trips. Penalized splines incorporate a penalty that drives the coefficients of non-contributing variables to zero (Wood 2006). These variables were removed after the first iteration, and then backward, stepwise selection was used on remaining variables using non-penalized splines, removing the variable with the highest *P*-value at each iteration until only variables with a *P*-value <0.001 remained (Zuur et al. 2009). We explored model structures in which individual smoothed variables were constrained using knots, as well as formulations leaving variables unconstrained. Knots determine the complexity and flexibility of the curve and can limit overfitting. Overall patterns and variable selection outcomes were similar for both strategies, but smooth terms were determined to be more realistic and interpretable when constrained to five knots, a common, conservative default. We present results only from the constrained version. Various other combinations of smoother types, parameter settings, and model selection algorithms were explored, without noticeable differences on the resulting inferences. The final, best-fit models from both interaction model and non-interaction model iterations were compared using AIC. All analyses were implemented in the package mgcv, version 1.8-31 (Wood 2006, 2007), in RStudio statistical software, version 1.2.5033 (R Core Team 2018).

Scale-dependent spatiotemporal analyses

We explored spatiotemporal patterns of depredation for all observed vessels simultaneously across a range of relevant space and time scales (maximum of 1000 km and 20 d). We first used a variation of Ripley's *K* function (Ripley 1977) to identify whether the occurrence of depredation exhibited spatiotemporal clustering across these scales. The technique treats the positions of specific events (e.g., depredation) as marked point processes to estimate the presence or absence of clustering of the event while controlling for the underlying distribution of all events (i.e., all fishing sets), as these are not randomly or evenly distributed themselves. By removing the effects of only space and only time, patterns of events due to space–time interactions can be identified (i.e., events that are close in both space and time). We also summarized the proportion of depredated or marked fishing events among all vessels fishing within specified times and distances from where the focal depredation event occurred (using the same space and time scales as the K-analysis). Space and time locations for these analyses were based on the beginning of the haul for all observed fishing deployments from 2004 to 2018.

For the clustering approach, we followed the approach of Dunn et al. (2014) and Bjorkland et al. (2015), applying the *K* function separately for all observed fishing deployments (all points, $\hat{K}(s, t, st)_{\text{all}}$) and observed depredated deployments only (marked points, $\hat{K}(s, t, st)_{\text{mark}}$), across a range of space–time thresholds (Gardner et al. 2008, Dunn et al. 2014):

$$\hat{K}(s, t, st) = \frac{AT}{N^2} \sum_{i=1}^{N} \sum_{j \neq i}^{N} \frac{I\left(\| s_i - s_j \| \leq d\right) I\left(\| t_i - t_j \| \leq t\right)}{w\left(s_i, s_j\right) v\left(t_i, t_j\right)}$$

where N is the total number of events, A is total area, T is total length of the time series, s_i is the spatial location of event i, t_i the time of event i, $w(s_i,s_j)v(t_i,t_j)$ an edge-correction factor, and I a function indicating events s_j,t_j within a distance s and time t of event s_i,t_i (Dunn et al. 2014). As the fishery operates on a daily time scale (i.e., typically one full set and haul per 24-h period), we used one day as our time interval, from a minimum of one day to maximum of 20 d. Similarly, as the gear can spread over tens of kilometers, we used 50 km as a minimum distance step and interval to a maximum of 1000 km. The maximum values for the distance and time steps were chosen to include all scales that could reasonably be considered actionable for mitigation purposes. We implemented $\hat{K}$ calculations in the Splancs package, version 2.01-40 (Bivand et al. 2017) in RStudio statistical software, version 1.2.5033 (R Core Team 2018).

We calculated both $\hat{K}(s, t, st)_{\text{all}}$ and $\hat{K}(s, t, st)_{\text{mark}}$ across each possible space–time interval. Purely spatial and temporal effects ($\hat{K}(s)$ and $\hat{K}(t)$; Appendix S2: Eqs. S1 and S2) for all fishing sets and depredated sets were then subtracted from the respective $\hat{K}(s, t, st)$ (Appendix S2: Eq. S3) to isolate processes correlated in both space and time only (i.e., space–time interactions). Finally, the space–time clustering of the full dataset was subtracted from that of the

marked points $\hat{K}(st)_{\text{mark}} - \hat{K}(st)_{\text{all}}$, to identify space–time effects of only the marked points (i.e., controlling for the nonrandom distribution of fishing events).

We then used random-labeling permutations to explore the spatiotemporal autocorrelation of depredation relative to randomly permuted fishing set events. This method builds envelopes of K by taking 1000 random samples of the same size as the number of marked points from the overall dataset. These envelopes represent the range of expectations of K if there were no space–time structure to the data. We consider observed Ks that exceed the highest 95% threshold of these values at a particular space–time threshold to exhibit clustering. We acknowledge concerns of this method for assigning statistical significance (Loosmore and Ford 2006), and we considered this only as a data exploration exercise to identify plausible scales of correlation. For visualization purposes, at each space–time threshold, we subtracted the value of the highest 95th percentile of permuted Ks from the observed K and set all zero (random) or negative values (overdispersed) to zero. We then divided these subtracted K values by the highest K value across all space–time scales to standardize on a scale from zero to one, and we display this as a heat map to visualize specific space–time thresholds where aggregation is likely present (Gardner et al. 2008, Dunn et al. 2014).

While the K function provides information on the intensity of spatiotemporal clustering at different scales, it does not translate directly to a quantitative understanding of the change in risk of depredation relative to an observed depredation event. Thus, we also summarized the occurrence of depredation as a function of space and time from an observed depredation event. Specifically, we calculated the empirical proportion of depredation (fraction of total sets that are marked), within each space–time boundary, for every observed depredation event. In other words, when depredation occurs, what is the average rate of occurrence of additional depredation on all other nearby vessels, within each space and time window of the original event? We note that this method does not isolate combined space–time effects like the K-analysis, and thus, independent time or space effects may be aggregated here as well, such as seasonal or static habitat correlates. To put these scales in context, we also explored the typical behavior of fishermen in response to interactions, calculating distances moved and time elapsed between sets (end of one haul to beginning of next set), following the presence or absence of odontocete depredation or false killer whale bycatch.

False killer whale movement analysis

Pelagic false killer whales were encountered and tagged with satellite tags during ship-based (Pacific Islands Fisheries Science Center, PIFSC) and small-boat (Cascadia Research Collective, CRC) cetacean surveys in 2013 (both), 2017 (PIFSC only), and 2020 (CRC only). See Appendix S3 in this paper, Baird et al. (2010), Baird et al. (2013), and Anderson et al. (2020) for further details on encounter, sampling, and tagging protocols. To avoid pseudo-replication, when multiple tags were deployed within a single group or animals tagged on separate days joined later, we included only the tag with the longest transmission time in subsequent analyses.

Filtered Argos data were further processed using a Correlated Random Walk state-space model (crw-ssm) using the foieGras package, version 0.4.0, implemented in RStudio version 1.2.5033 (R Core Team 2018) as described in Jonsen and Patterson (2019). The Correlated Random Walk model is a continuous time model that accounts for the irregular time intervals between positions available from Argos data. It estimates true locations while accounting for error in the Argos telemetry data and regularizing to consistent, pre-specified time intervals, in this case 4 h. This allows data across multiple individuals to be normalized and as comparable as possible. False killer whale locations were regularized to four-hour intervals for up to the first 59 d after which tags began duty-cycling. We then summarized horizontal distance moved and average speed along four-hour interval tracks and horizontal distance moved, speed, and total displacement (straight-line distance from the first location of each day to the first location of the following day) for daily time steps.

Results

Between 2004 and 2018, a total of 267,231 sets (mean 17,815 per year, standard deviation [SD]

1357) were made on 20,262 trips (mean 1351 per year, SD 97) by 187 unique vessels (mean 132 per year, SD 7) in the Hawai'i deep-set longline fishery. Observers were present on 21.0% of trips covering 20.7% of sets, providing a dataset of 55,247 sets (mean 3683 per year, SD 254) with detailed data. Fishermen set an average of 13.3 sets per trip (SD 3.7) and 2355 hooks per set (SD 455.5) with an average soak time (end set to end haul) of 15.2 h (SD 2.8). Odontocete depredation on at least one captured fish was observed on 3478 (6.3%) of all observed sets. Approximately half of trips (47.2%) experienced odontocete depredation on at least one set and 21.2% experienced odontocete depredation on two or more sets. The number of fish depredated per set was right-skewed, with a median of two and a maximum of 63 depredated fish recorded on sets with depredation. Odontocetes depredated a variety of fish species, mostly tunas (*Thunnus* spp., 68%), followed by billfish (11%), mahi-mahi (6%), and wahoo (5%). These species represented 28%, 4%, 8%, and 2% of total catch, respectively. Several species were depredated infrequently relative to their proportion of total catch. Notably, the most frequently caught species in this fishery, the longnose lancetfish (*Alepisaurus ferox*), comprised 23% of fish caught by number but less than 2% of fish depredated by odontocetes. This may be due to avoidance by odontocetes or the gelatinous nature of their flesh, which makes this discard species easily damaged and difficult for observers to categorize the source of damage. In general, odontocetes did not feed on captured sharks. The blue shark (*Prionace glauca*) is the third most frequently caught species (~8% of total catch), but only seven individual sharks of three species had evidence of odontocete depredation.

A diverse range of cetacean species were reported as hooked or entangled by observers, but most were odontocetes in the family Delphinidae (152 of 158 total animals). The most commonly caught cetacean was the false killer whale, representing approximately 70% of all bycaught cetaceans identified to species or genus (122 total). In total, 85 confirmed false killer whales were caught on 80 sets between 2004 and 2018, followed by 10 short-finned pilot whales (*Globicephala macrorhynchus*), nine Risso's dolphins (*Grampus griseus*), and seven common bottlenose dolphins (*Tursiops truncatus*). There were also 13 unidentified blackfish species, likely false killer whales or short-finned pilot whales (McCracken 2010). Depredation of catch was observed on 51 of 80 (~64%) sets in which one or more false killer whales were hooked.

Multivariate analysis

We used GAMMs to predict the presence or absence of odontocete depredation per set (occurrence of ≥ 1 depredated fish or false killer whale bycatch event as a proxy for depredation) as a function of variables hypothesized to influence interaction rates. The parameters included in the best-fit final models, and their functional relationships to depredation, were very similar for each model type (i.e., with interactions and with no interactions; Appendix S1: Eqs. S3 and S4). The main differences were that the month × latitude interaction term was significant in the interaction model and distance to seamount was marginally significant in the no-interaction model, but not kept in the interaction model. The interaction model had the lowest AIC value and highest deviance explained and thus was considered further. The final interaction model included the interaction between month and latitude, 11 additional quantitative variables, one categorical variable, and a random vessel identification effect, although overall deviance explained was still low at 8.11% (Table 1; Fig. 1). There was a clear seasonal and spatial relationship, with a decrease in depredation occurrence in the second and third quarters of the year and at higher latitudes. Of the ONI variables, only the 11-month lagged version was kept in the final model and was positively associated with depredation. The only other significant oceanographic variable was a positive relationship between depredation and absolute dynamic topography.

Operationally, the probability of depredation increased with the number of hooks set and more time the gear spent in the water. Depredation was also significantly more likely if the vessel experienced depredation on the previous haul of the same trip. These factors led to relatively large shifts in the model-predicted probability of depredation. For example, the predicted probability of depredation more than doubled when fishermen set 3000 vs. 1500 hooks or when depredation occurred on the previous set. Finally, several catch-related variables were

Table 1. Results for the best-fit GAMM predicting odontocete depredation rates in the Hawai'i deep-set longline fishery from 2004 to 2017.

Term	Estimates	SE	edf	χ^2	P
Parametric terms					
Intercept	−3.04	0.03			<0.001
Depredation on previous set	0.90	0.06			<0.001
Smoothed terms					
Latitude × Month			14.0	302.10	<0.001
No. hooks set			1.91	110.93	<0.001
Soak time (h)			2.35	30.26	<0.001
Bigeye tuna (no. caught)			3.93	379.51	<0.001
Yellowfin tuna (no. caught)			2.85	54.08	<0.001
Mahi-mahi (no. caught)			3.46	32.25	<0.001
Wahoo (no. caught)			2.06	27.61	<0.001
Sharks (no. caught)			1.00	17.39	<0.001
CPUE (no. fish/1000 hooks)			3.89	73.69	<0.001
Nearby tuna CPUE (no. tuna/1000 hooks)			3.49	141.22	<0.001
ONI 11 months Lag			1.00	19.83	<0.001
Absolute Dynamic Topography (m)			1.00	28.71	<0.001
Vessel ID			65.95	124.16	<0.001

Notes: The abbreviation "edf" is the estimated degrees of freedom in GAMM fitting.
n = 49,579; R^2 (adj.) = 0.048; Deviance explained = 8.11%; UBRE = −0.571.

significant. There was a consistent, nonlinear relationship between depredation and catch of four of the most common target species (bigeye and yellowfin tuna, mahi-mahi, and wahoo) in which the likelihood of depredation decreased with increasing catch and then leveled off or increased again at high levels of catch. Overall CPUE (number of bony fish per 1000 hooks on the focal vessel) showed the same relationship, while average, tuna-only CPUE on vessels setting within 100 km and ±1 d had a linear, positive association with the risk of depredation. Number of sharks caught also had a linear, positive relationship with depredation occurrence, and vessel ID was highly significant as a random effect.

Scale-dependent spatiotemporal analyses

The GAMM results showed an increased probability of depredation when a vessel experienced depredation on their prior set of the same trip. The modified Ripley's K method allows further exploration of this pattern by considering the occurrence of depredation across all co-occurring vessels that are close in space and time. This analysis showed a clear, spatiotemporal aggregation of depredation occurrence at most scales up to 1000 km and 20 d (Fig. 2a). The peaks in this surface indicate where clustering or aggregation is most intense—these occurred over areas of between 350 and 450 km and periods of 9–11 d. Our summary of empirical, or observed, depredation rates relative to distance and time since previous depredation events is consistent with the indicated spatiotemporal clustering. The observed depredation rate was 18% for vessels setting less than 50 km and 24 h from previous depredation, but this rate dropped the farther away a vessel fished from a previous encounter. At the peaks from the Ripley's K, roughly 400 km and 9 d, the empirical depredation rate flattened to about 9% (a 50% reduction) and there was little additional benefit from moving farther (Fig. 2b). Empirical depredation rates declined somewhat more rapidly with distance than time from the observed event, such that increased risk may be persistent for several days or more.

The analysis of fishermen behavior showed that, in the absence of odontocete interactions, fishermen moved a median 35 km (interquartile range [IQR] 16–64 km) with a median duration of 4.3 h (IQR 2.9–6.1 h) from the end of that haul to the beginning of their next set. If depredation was experienced on a haul, they moved a median 46 km (IQR 24–83 km) in 4.7 h (IQR 3.2–7.3 h)

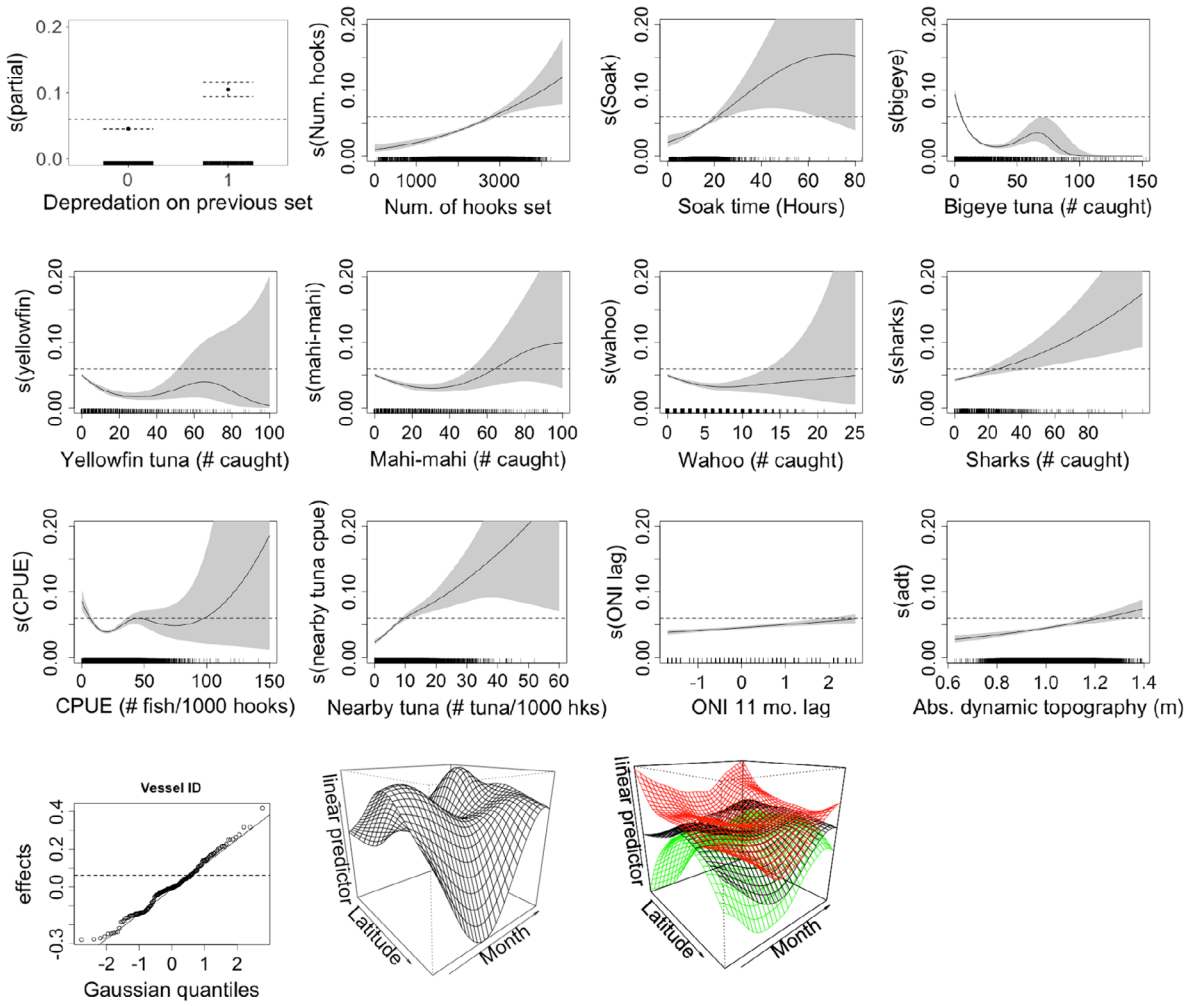

Fig. 1. Smooth and parametric functions for variable output in binomial GAMM of depredation occurrence. Figures represent presence/absence of odontocete depredation as function of each variable when all others are at their average value. *Y*-axis values are transformed from log-odds to probability scale and shifted by the model intercept to represent expected probability when all other variables are at their average value. The overall model-predicted probability (˜0.06) of depredation is indicated by a dashed line in each figure so that the influence of each variable on probability of depredation can be directly assessed and compared. Distribution of observed values indicated by rug plot along *x*-axis. Shading reflects 2× SE curves. Interaction term indicated by topographic perspective plot. Red/green indicate ± 2 SE.

before starting the next set, and 61 km (IQR 34–205 km) in 5.8 h (IQR 3.5–25.3 h) if a false killer whale bycatch event occurred.

False killer whale movement analysis

Tags were deployed on eight pelagic false killer whales during six encounters in 2013, 2017, and 2020. CRC deployed three tags in a group of approximately 16 individuals on 22 October 2013 and one tag in a group of 48 individuals on 14 May 2020 off of Hawai'i Island. PIFSC deployed one tag in a group of an estimated 23 individuals on 15 May 2013 and one tag in a group of estimated 15 individuals on 26 May 2013, both in the NWHIs. PIFSC deployed an additional two tags near the island of Kaua'i, one in a group of

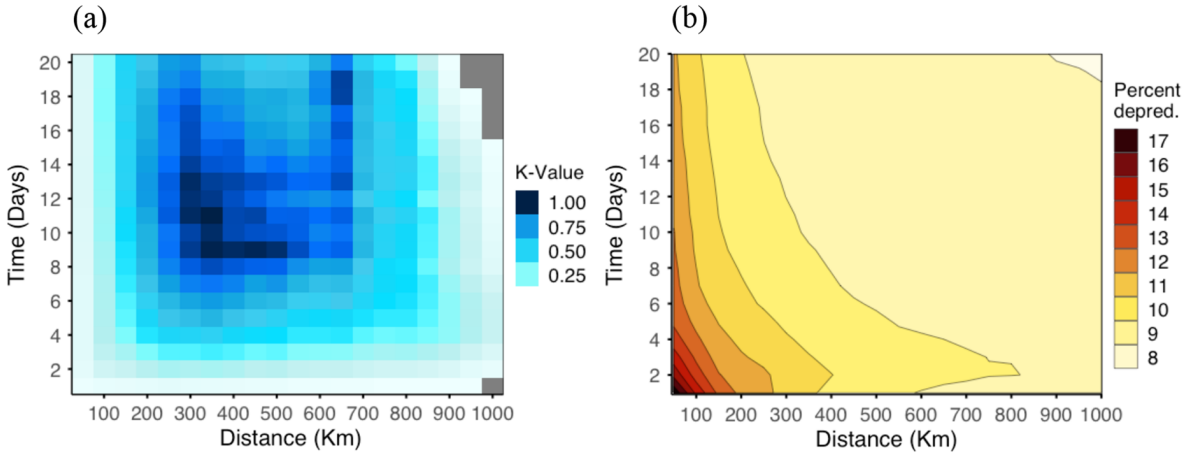

Fig. 2. (a) Spatiotemporal clustering of odontocete depredation in the Hawai'i deep-set longline fishery from 2004 to 2018 represented by modified Ripley's K. Colored tiles are relative strengths of clustering, with any color-shaded tile (i.e., non-gray) representing spatiotemporal clustering above 95% random permutations at that space–time scale. The highest values represent the strongest levels of spatiotemporal clustering. (b) Percent occurrence of odontocete depredation based on time and distance (begin of haul) from a previous depredation event in the Hawai'i deep-set longline fishery.

approximately 32 individuals on 12 September 2017 and one in a group of approximately 19 individuals on 13 September 2017. Total tag durations, geographic use, and potential direct interactions with pelagic longline operations for the whales tagged in 2013 are described in greater detail in Anderson et al. (2020).

There were five independent tags, with two (PcTagP02 and PcTag065) transmitting for about two weeks and the other three (141702, PcTag041, and PcTagP01) transmitting beyond the 59 d of daily transmissions considered here (Fig. 3). We included only full days of transmission, leaving 12 d for PcTagP02, 15 d for PcTag065, and 57 d each for the longer three (Table 2). Total distance traveled ranged from 1653 km in 12 d for PcTagP02 to 8099 km in 57 d for tag 141702. Median distance traveled in 4 h for all animals was 19 km (range 1–75 km), translating to a median speed of 4.8 km/h (range 0.3–18.8 km/h; Table 2, Fig. 4). When considered at the daily scale, animals moved a median distance of 117 km (range 64–335 km) and median speed of 4.9 km/h (range 2.7–14.0 km/h). Median displacement (straight-line distance from first location of day to first location of following day) was 81 km (range 2–333 km).

Discussion

We used several complementary approaches to explore patterns of odontocete depredation in the Hawai'i deep-set longline fishery. We first utilized a large observer dataset to explore relationships between odontocete depredation and environmental and operational covariates concurrent with deep-set fishing activity. These model outcomes largely corroborated those from an earlier analysis (Forney et al. 2011), with the larger dataset allowing for increased resolution of several patterns. The model did not identify environmental or operational covariates that could be used in a predictive management context, but it showed that the risk of depredation doubled if the previous set on the same trip experienced depredation. We explored whether the occurrence of depredation on other, nearby vessels also influenced depredation risk and identified the space and time scales of such repeat depredation to understand how risk changes with proximity to observed interactions. We also summarized false killer whale travel speeds and distances derived from satellite tags to help contextualize these scales of depredation and understand how movement of the depredating species

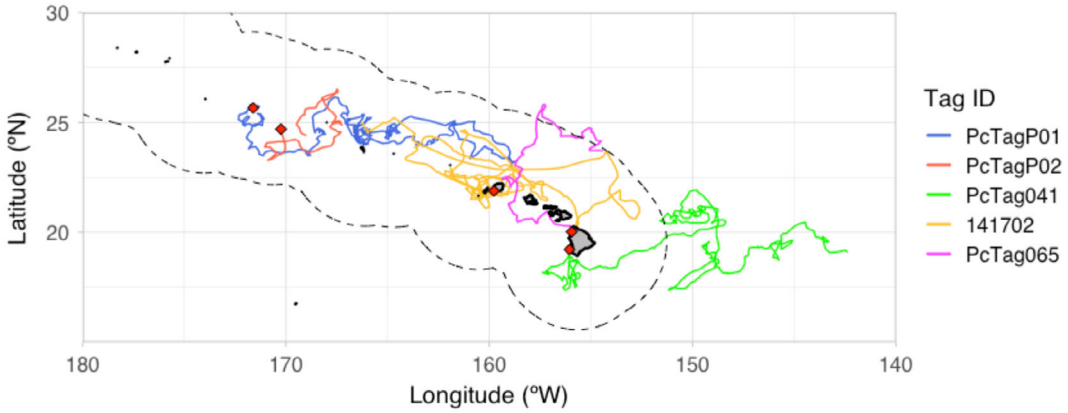

Fig. 3. False killer whale satellite tag tracks. Red diamonds indicate tag-on locations. Dashed line represents the U.S. EEZ around the Hawaiian Islands. See text and Table 2 for further details.

Table 2. Details on pelagic false killer whale tag deployments considered in movement analysis after filtering through Douglas Argos-Filter and Correlated Random Walk state-space model.

					Distance traveled (km)†		
Tag ID	Deployed by	Deploy date	End date	No. days	Cumulative	In 4 h	Daily
PcTagP01	PIFSC	16 May 2013	2013-07-13	57	6705	18 [2–54]	113 [64–203]
PcTagP02	PIFSC	27 May 2013	2013-06-09	12	1653	21 [2–44]	125 [71–169]
PcTag041	CRC	22 October 2013	2013-12-19	57	6602	17 [1–63]	112 [65–192]
141702	PIFSC	12 September 2017	2017-11-09	57	8099	21 [1–75]	129 [64–335]
PcTag065	CRC	15 May 2020	2020-05-31	15	2001	21 [4–49]	121 [105–149]

† Distance traveled in 4 h and daily are expressed as median with range in square brackets.

contribute to the patterns we observed. Our analyses provide specific guidance on how fishermen can reduce the probability of repeated interactions following a depredation or bycatch event. Thus, our results have direct relevance to the ongoing deliberations of the False Killer Whale TRT and may inform management of other odontocete–longline interactions.

GAMM analysis of environmental and operational covariates

The overall explanatory power of the best-fit model was low, but several clear patterns emerged from the multivariate analysis of depredation occurrence. There was a marked decrease in interaction rates during the second and third quarters of the year and at higher latitudes, beyond around 18°–20° N (Fig. 1). This pattern was also observed by Forney et al. (2011) and is to be expected as the fleet extends north and east in these months (Woodworth-Jefcoats et al. 2018) into areas where false killer whale densities are predicted to be the lowest for this region of the Pacific (Forney et al. 2015, Bradford et al. 2020). Depredation is generally lowest at the northernmost extent of fishing effort, but it seemed to decrease at all latitudes during the Northern Hemisphere summer months (Fig. 1). False killer whales likely move seasonally in response to changes in sea surface temperature (Bradford et al. 2020), and this could influence the intensity of overlap with fishing activity across the fleet's range. We also note that, although bycatch records and direct observation (Thode et al. 2016) suggest that false killer whales are the primary depredator species in this fishery, some depredation observations are likely due to other odontocete species. These broad space and time patterns may thus be partially influenced by interactions between these species' ranges, environmental conditions, and fishery behavior that cannot be disentangled here.

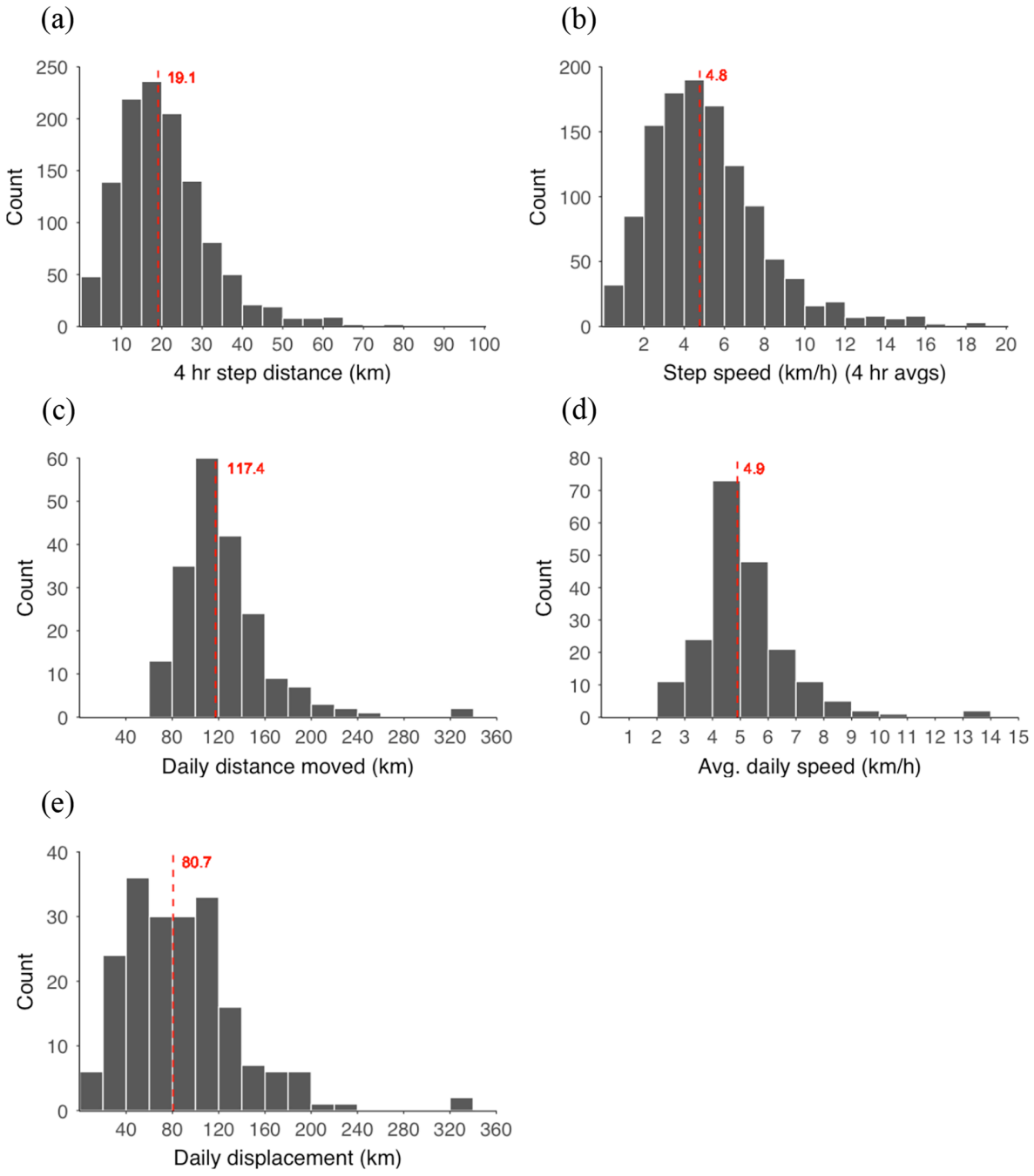

Fig. 4. Summary histograms of sub-daily (4-h) track-line distance traveled and speed (a, b), daily track-line distance and speed (c, d), and total daily displacement (e) from five pelagic false killer whale satellite tags processed through Douglas Argos-Filter and Correlated Random Walk state-space models. Red values indicate median.

Depredation occurrence increased with absolute sea surface height, which is an indication of mesoscale features such as eddies and fronts (Chelton et al. 2011). This may relate to higher depredation in more productive habitats along these features, which is consistent with the higher depredation rates observed when target species CPUE is high. We also documented a

possible relationship between odontocete depredation and ENSO conditions. A weak but significant positive correlation (~0.14) was detected between the Oceanic Niño Index (ONI) and depredation 11 months later (Appendix S1: Fig. S1), and this lagged ONI value was significantly positively associated with depredation rate in the GAMM analysis. It is unclear what ecological processes underlie this pattern. There could be a seasonal correlation component as El Niño events (ONI $\geq$ 0.5) disproportionately occurred in quarters 1 and 4 when there were higher rates of depredation. However, La Niña events (ONI $\leq$ −0.5) had a similar monthly distribution to El Niño and yet La Niña was associated with low depredation rates. A seasonal pattern would also not likely account for the apparent yearly fluctuations, and interaction terms between ONI lag and month and ONI lag and latitude were not significant in the depredation models. Strong El Niño events are known to disrupt oceanographic conditions and marine food webs, although effects on upper trophic level predators are not well understood (Lehodey et al. 1997, Stenseth et al. 2002). Perhaps false killer whales opportunistically target fishing vessels more frequently when El Niño periods destabilize their normal food webs, and this occurs at the observed lag due to impacts taking time to move through the prey community. However, it would be very difficult to empirically test this hypothesis and, for now, we simply note the pattern.

Operationally, we observed that the probability of depredation increased with number of hooks set and soak time in hours. Indeed, fishermen could reduce their risk by approximately 50% (~0.06 to ~0.03) by making sets <1500 hooks or completing the haul in less than 10 h. Soak time and the amount of gear have similarly been observed to influence depredation rates in demersal longline fisheries (Tixier et al. 2015*b*, Janc et al. 2018), reinforcing that simple strategies that reduce depredator access can be beneficial in reducing interactions. We also observed relationships between depredation and a number of catch indicators. For four of the most common target species, there was a similar, nonlinear relationship in which the probability of depredation decreased with catch and then leveled off at low probabilities or increased back to more neutral effects at high catch rates. We also observed an increase in the probability of depredation as the CPUE of tuna species by all vessels within 3 d and 200 km increased, as well as with the number of sharks caught. These patterns suggest that depredation is more common in areas where CPUE is high, which is to be expected, given false killer whales are apex predators that target many of the same species as the fishery (Baird et al. 2008). Most of the commonly caught shark species in this fishery are also apex predators and may similarly be drawn to regions that are favored by false killer whales. The nonlinear patterns at the focal vessel may be explained by generally low catch rates when depredation occurs. False killer whales are known to depredate bait in the deep-set fishery (Thode et al. 2016, Bayless et al. 2017), which could depress overall catch rates. The fish heads counted by observers are also an imperfect indicator of depredation, and it is possible that the whole fish is sometimes removed by the depredating whale or falls off the line before the hook is hauled. This would also be consistent with the more linear trend for sharks, as sharks are almost never depredated by odontocetes (see also Oleson et al. 2010). The uptick in depredation at very high catch levels may be associated with the general pattern of false killer whales occurring in relatively productive areas.

Spatiotemporal depredation patterns

The GAMM shed light on finer scale patterns of depredation as well, such that depredation was significantly more likely if a vessel experienced depredation on the previous set of its same trip. This is consistent with the results reported by Forney et al. (2011) and reports from fishermen (TEC 2009), which suggest fishermen experience repeat depredation on trips and may actively move following depredation to reduce the probability of repeat occurrences. Forney et al. (2011) suggested that moving 100 km following a depredated set leads to slight reductions in risk (from 16% to 14% expected occurrence), but there was insufficient sample size in their analysis to assess time and space together and only interactions on the focal vessel were considered (i.e., not what is happening on other, nearby vessels).

We addressed these gaps using a variation of Ripley's K to estimate spatiotemporal

autocorrelation of depredation simultaneously for all vessels across a range of actionable space and time scales. This approach has been used in other fisheries experiencing depredation or bycatch to identify scales of clustering, which can then be used to provide recommendations of distances to move, and/or times to wait, to avoid future negative encounters; these are commonly referred to as move-on rules. We identified spatiotemporal clustering of depredation in the deep-set fishery across most scales we considered, suggesting that a vessel should generally expect to encounter higher depredation rates near previously observed depredation events due to spatiotemporal clustering of events alone (i.e., independent of any effects of just time or just space).

To give a clearer picture of what fishermen could actually expect in terms of risk of depredation relative to the time and location of previous depredation, we also identified the average proportion of sets experiencing depredation (for all vessels simultaneously) within the same space–time thresholds from the observed depredation event (i.e., within 20 d and 1000 km at increments of 24 h and 50 km). As for a single vessel, the rate of depredation across all vessels is highest when a previous depredation event is observed nearby in space and time. On average, the proportion of sets experiencing depredation within 24 h and 50 km of a previously observed depredation event is ~18%, compared to the overall background rate of ~6%. Consistent with the *K*-analysis, this proportion decreases with both space and time since the observed event. The peaks from the *K*-analysis indicate that ~400 km and ~9 d is the most effective distance to move and time to wait, respectively, for reducing repeat depredation. On average, the depredation rate decreased from 18% to 9% (~50% reduction) at this threshold, with little additional benefit gained by moving farther or waiting longer.

There also seems to be a greater benefit from moving rather than waiting, suggesting that these clusters of depredation activity may be relatively confined in space (still potentially over several hundred km), but persistent in time (i.e., lasting for up to several weeks). This may be beneficial to the fleet, as moving is likely to be a more practical strategy than simply waiting without fishing, although there are obvious costs associated with both. Indeed, past fishing practices suggest that pelagic longline fishermen tend to react to depredation and bycatch by moving but fishing again as soon as possible. Fishermen moved around 31% farther between sets when they experienced odontocete depredation and 74% farther when there was a false killer whale bycatch event, but the median times for each scenario were all under six hours, indicating a tendency to move but still set on the same day (so that a potential fishing day was not missed). We also note, however, that although the median times are similar, the upper quartile of time between sets increased to >24 h following a false killer whale bycatch event, suggesting that at least some vessels or captains may be likely to both move and wait an extra day before fishing again. The *K*-analysis does suggest that any movement farther from an observed interaction will decrease the likelihood of repeat occurrences, but based on our move-on analysis, the distances typically moved may provide only very minor benefits when fishing again within 24 h. For example, the average percentage of depredated sets within 61 km and 24 h of a previously observed depredation event was 17% (compared to 18% within 50 km and 24 h), while this decreased to 12% on the same day but 200 km away.

Depredator behavior and avoidance

The incidence of depredation is ultimately driven by the behavior of the depredator, and there have been important recent advances in understanding the nature of interactions between false killer whales and the Hawai'i deep-set longline fleet, and for interactions with odontocetes in other fisheries. For example, passive acoustic monitoring of longline gear deployments detected false killer whales most commonly during the hauling phase, with whales potentially moving along the mainline away from the vessel as gear was being retrieved (Bayless et al. 2017). Satellite-tagged false killer whales were also observed to show directed movements toward fishing gear during the hauling phase of some sets (from as far as 100 km away) and no apparent reaction to gear during other sets, despite being within apparent detection range (Anderson et al. 2020). It is still unclear how false killer whales locate gear, although work with other

species and fisheries suggests that acoustic detection is very likely. Thode et al. (2007) showed that sperm whales depredating demersal longlines in southeast Alaska cue in on acoustic signatures from the cavitation of a ship's propeller when the engine is engaged to begin hauling gear, which they can detect from at least 4–8 km away. Thode et al. (2015) further point out that sperm whale clicks are more intense than the vessel noises themselves, and thus, once at the gear location, depredating sperm whales may intentionally or unintentionally alert other whales from even farther away. Richard et al. (2021) recently identified clear acoustic signatures during setting operations of demersal longlines in a sub-Antarctic fishery. They argue that there may be multiple acoustic cues available to depredating whales for a given fishery and that different cues may travel different distances. This may help explain observations that killer whales in South Georgia orient to demersal longlines at 75–100 km (Towers et al. 2019), while they seem to orient to herring purse seine vessels in Norway when within 20 km (Mul et al. 2020).

Taken together, these studies demonstrate that false killer whales are likely capable of locating vessels from tens of kilometers away, following vessels, and moving along gear removing bait and target catch once found, although they do not always do so. Our spatiotemporal analysis identifies clear space–time aggregation of longline depredation, which could be a result of this type of active targeting and following of vessels by whales, simple overlap of whales, and vessels targeting similar dynamic oceanographic conditions or, more likely, some combination of both. We provide a summary of baseline pelagic false killer whale movement behavior, using the same tags as Anderson et al. (2020) plus an additional tag from PIFSC in 2017 and CRC in 2020, to place in context the mobility of these pelagic predators and provide guidelines for what would be required to avoid or escape whales that are actively pursuing a vessel.

Over four-hour time periods, comparable to the typical duration between the end of a deep-set haul to beginning the next set, the median distance moved by the five focal whales was 19 km (median speed of 4.8 km/h). However, all five whales moved over 40 km in a four-hour period (speed of 10 km/h), two were observed to move over 60 km (15 km/h), and one exceeded 70 km in four hours on three different days (17.5 km/h). This compares to kinematic predictions of false killer whale speed based on morphology and cost of locomotion, which suggest cruising speeds of 11 km/h and highest efficiency of swimming at 13–14 km/h (Fish 1998). Burst speeds are likely much greater than could be maintained over four hours. Fish (1998) estimated maximum velocities for false killer whales of 27 km/h and Baird (personal observation) observed a group of false killer whales near Hawai'i maintaining speeds of 18 km/h for over 30 min.

Over daily time periods, the median along-path distance was 117 km with a median speed of 4.9 km/h. However, distributions were again right-skewed with whales observed to move well over 200 km in 24-h periods, maintaining speeds of at least 10 km/h. We note that reported along-path distances are all minimum values as whales are unlikely to move in straight lines for four or 24 h. More accurate GPS-based tags, as well as better estimation of false killer whale cost of transport and aerobic capacity, could further inform how long animals are able to maintain high cruising speeds and how long they might be expected to pursue vessels.

False killer whales have a complex social structure, and groups are often comprised of multiple sub-groups spread over distances up to at least 35 km (Baird et al. 2008, Bradford et al. 2014, Martien et al. 2019). Individuals within groups have been observed separating by over 100 km and rejoining the same group over a period of several days (Baird et al. 2010). Assuming a minimum detection range of 4–8 km for vessel noise and no movement by the depredating whales, it is thus possible that a vessel would have to move 40–50 km (acoustic propagation of vessel noise + spread of sub-groups) just to reach the edge of detection range for a large group of false killer whales. This distance could, of course, increase if individual whales disassociate and reassociate as observed by Baird et al. (2010) or follow the vessel as it moves to a new fishing location, which is known to occur in other odontocete–fishery interactions. Tixier et al. (2015*b*) demonstrated that a single pod of killer whales (*Orcinus orca*) could follow longline vessels for multiple days and suggest that the whales may even maintain their

bearing, such that they can encounter and depredate gear several days later, despite likely losing contact with the acoustic signal of the vessel.

How long a vessel would have to move to outpace following whales depends on the speeds of the vessel and whale. The average maximum speed of Hawai'i longline vessels is about 15 km/h (obtained from MarineTracker.com), which is similar to the maximum speeds maintained in four hours by tagged false killer whales. Thus, it is possible that a vessel at maximum speed could still have following whales after four hours. Even if whales were moving at 10 km/h, which all tagged whales were easily capable of, a vessel moving at 15 km/h would only be 20 km from the following whales after four hours. As it could take three hours just to reach the conservative edge of detection range of 40–50 km, whales may be able to maintain detection well beyond four hours, even if the vessel moves at maximum speed. Our spatiotemporal analysis suggests that when fishing again within one day, vessels are unlikely to experience large decreases in depredation risk unless they move fairly large distances. We recognize constraints may limit a vessel's ability to move certain distances. Deep-set gear is typically deployed (set) in the morning with haul-back beginning around sunset and finishing in the early morning hours. A captain who wishes to fish two days in a row typically has only a few hours to redeploy gear at the optimal time of day, hence the median of ~4 h from end of haul to beginning the next set. Unfortunately, even at the average maximum speed for these vessels, fishermen are unlikely to decrease their interaction risk within only four hours. We thus recommend that when depredation is known to occur, vessels move away as far and as quickly as practical. It may also benefit to diverge from the course of travel for 10–20 km before setting gear, as false killer whales may behave like killer whales and continue following in one direction after losing acoustic detection of the vessel (Tixier et al. 2015*b*). Vessels will experience greater reduction in risk if they wait to set until the following fishing day.

Recommendations and implications

Our work was motivated by the goal of identifying patterns of odontocete depredation and depredator behavior in a way that can be used by fishermen to mitigate these negative interactions. We detected some interesting patterns, but there were no unequivocal geographic, environmental, or operational covariates that could be used in a management context. As has been shown before, the probability of interaction increases with fishing effort (hooks set and time soaked). But, in general, odontocete depredation is likely driven at broad scales by convergence in space and time of fishing activities and the occurrence of these apex predators, which are both targeting similar prey fields. Both fishermen and whales are likely cueing on the same set of environmental factors to locate these areas. Nevertheless, depredation is still a relatively rare event, and thus, high predictive accuracy based on a priori environmental factors alone is not currently possible.

Given the clumped occurrence of this behavior in space and time, it is not surprising that the best predictor of depredation is where and when it was observed previously. We characterize the boundaries of risk associated with previously observed events, which suggest that depredation risk consistently decreases until about 9 d later and 400 km away, with little expected reduction beyond that. Risk seems more persistent in time than in space. For example, the same proportion of sets were depredated within 50 km and 8 d of a depredated set than within 200 km only one day later. Thus, if vessels wish to fish again within 24 h, they will experience the greatest reduction in risk by moving or staying as far away as possible, ideally 200–300 km.

We further considered the behavior of tagged pelagic false killer whales. False killer whales can pace fishing vessels for at least four hours. We recommend that fishermen steam at high speeds (>15 km/h) for seven to eight hours if setting the same day, but again, they will experience further benefit if they wait until the next day to fish, allowing time to move even farther. This may be challenging under typical fishing operations, so fishermen who intend to fish on consecutive days may be able to capitalize on synergies between the reduction of risk at lower fishing effort and greater distances moved following depredation. By setting slightly less gear they should finish hauling earlier in the day. If depredation were to occur on that haul or be known to have occurred recently in their area, they would

thus have more time to move to a safer location on the same day.

We also showed that risk is increased for all vessels in the vicinity of known interactions, suggesting that improved communication among vessels in the fleet would help reduce risk (Gilman et al. 2006). It may be difficult for a vessel at the center of a group of whales to escape detection within a day, but other vessels fishing in the same area can use that knowledge to reduce their own risk. Elevated depredation risk may persist within 100–200 km for a week or more, so it is important for other vessels to know where interactions occur so that they do not inadvertently fish again within high-risk areas. We understand that competition may reduce incentives to communicate among some vessels, and cooperation may be even less likely outside of the U.S. EEZ, where vessels from a number of other nations may also be longline fishing. However, reducing bycatch risk is in the best interest of all U.S. fleet members, given the potential management implications of high bycatch rates.

Finally, we recognize that although moving and waiting reduce odontocete interaction risks, they also incur costs themselves. Ultimately each captain must make decisions based on the perceived costs and the benefits of moving versus continuing to fish. We have attempted to provide information to help them evaluate part of this calculation, specifically the expected risk reduction from given avoidance measures. We hope that they can use this information to more precisely evaluate the trade-offs in adopting these recommendations. Further work assessing the costs in terms of lost fish catch would be beneficial in helping fill in additional parts of these calculations that are not addressed here.

Depredation and associated bycatch are global issues but remain poorly understood in many ways, especially for pelagic longline fisheries where depredating animals are rarely seen in the vicinity of gear. Our study adds to a growing body of work for the Hawai'i longline fleet but is also relevant to pelagic longline depredation in other parts of the world. Unfortunately, depredation and bycatch will be difficult to avoid whenever the predators and fisheries target the same species. However, for species that occur in low densities with relatively low interaction rates, such as false killer whales, it may be possible to avoid areas of overlap and find other productive grounds to fish without whales. The tools used here can help identify the intensity and scale of risk where whales are known to occur, and the avoidance strategies most likely to be effective in minimizing further risk to the fishery. We demonstrate that rates of interaction can be reduced by up to 50% with appropriate avoidance measures. We hope that fishermen will add these measures to their toolkit for deciding where to fish, reducing economic burdens on the fleet, and improving conservation outcomes for vulnerable bycatch species.

Acknowledgments

We gratefully acknowledge funding support for JEF from the National Oceanic and Atmospheric Association's (NOAA) Fisheries Bycatch Reduction Engineering Program (BREP) [grant number NA17NMF4720261] and the Duke University Graduate School. We thank the Pacific Islands Regional Observer Program, especially their fisheries observers, who collect the data essential for documenting patterns of depredation and bycatch in Hawai'i longline fleets. We are very grateful to Christophe Guinet, who provided important discussion and advice on methods, resources, and office space to JEF to conduct parts of this analysis and helpful feedback on an earlier version of this manuscript. We thank Daniel Webster, Colin Cornforth, and Alan Ligon for tag deployments and the crew and researchers on the NOAA ship *Oscar Elton Sette* and the CRC field staff who provided logistical support for tagging efforts. We also thank Michaela Kratofil, Jason Roberts, and members of the False Killer Whale Take Reduction Team for providing valuable analytical advice and/or feedback on early results. We are also grateful for constructive feedback from two anonymous reviewers that greatly improved the manuscript. Research was conducted under NMFS permits Nos. 15330, 15240, 20311, and 20605. PIFSC research occurring in the Papahānaumokuākea Marine National Monument in 2013 was covered under permit PMNM-2013-001. This project received funding under award [NA17NMF4720261] from NOAA Fisheries Service, in cooperation with the Bycatch Reduction Engineering Program. The statements, findings, conclusions, and recommendations are those of the authors and do not necessarily reflect the views of NOAA Fisheries.

Literature Cited

Allain, V., J.-A. Kerandel, S. Andréfouët, F. Magron, M. Clark, D. S. Kirby, and F. E. Muller-Karger. 2008.

Enhanced seamount location database for the western and central Pacific Ocean: screening and cross-checking of 20 existing datasets. Deep Sea Research Part I: Oceanographic Research Papers 55:1035–1047.

Anderson, D., R. W. Baird, A. L. Bradford, and E. Oleson. 2020. Is it all about the haul? Longline fishery interactions and spatial use by pelagic false killer whales in the central North Pacific. Fisheries Research 230, 105665.

Baird, R. W., A. M. Gorgone, D. J. McSweeney, D. L. Webster, D. R. Salden, M. H. Deakos, A. D. Ligon, G. S. Schorr, J. Barlow, and S. D. Mahaffy. 2008. False killer whales (*Pseudorca crassidens*) around the main Hawaiian Islands: long-term site fidelity, inter-island movements, and association patterns. Marine Mammal Science 24:591–612.

Baird, R. W., E. M. Oleson, J. Barlow, A. D. Ligon, A. M. Gorgone, and S. D. Mahaffy. 2013. Evidence of an Island-Associated Population of False Killer Whales (*Pseudorca crassidens*) in the Northwestern Hawaiian Islands. Pacific Science 67:513–521.

Baird, R. W., G. S. Schorr, D. L. Webster, D. J. McSweeney, M. B. Hanson, and R. D. Andrews. 2010. Movements and habitat use of satellite-tagged false killer whales around the main Hawaiian Islands. Endangered Species Research 10:107–121.

Bayless, A. R., E. M. Oleson, S. Baumann-Pickering, A. E. Simonis, J. Marchetti, S. Martin, and S. M. Wiggins. 2017. Acoustically monitoring the Hawai'i longline fishery for interactions with false killer whales. Fisheries Research 190:122–131.

Bayse, S. M., and D. W. Kerstetter. 2010. Assessing bycatch reduction potential of variable strength hooks for pilot whales in a western north Atlantic pelagic longline fishery. Journal of the North Carolina Academy of Science 126:6–14.

Bigelow, K. A., D. W. Kerstetter, M. G. Dancho, and J. A. Marchetti. 2012. Catch rates with variable strength circle hooks in the Hawaii-based tuna longline fishery. Bulletin of Marine Science 88:425–447.

Bigelow, K., M. K. Musyl, F. Poisson, and P. Kleiber. 2006. Pelagic longline gear depth and shoaling. Fisheries Research 77:173–183.

Bivand, R., B. Rowlingson, P. Diggle, G. Petris, and S. Eglen. 2017. Package 'splancs': spatial and space-time point pattern analysis. https://cran.r-project.org/web/packages/splancs/

Bjorkland, R., D. C. Dunn, M. McClure, J. Jannot, M. A. Bellman, M. Gleason, and K. Schiffers. 2015. Spatiotemporal patterns of rockfish bycatch in US west coast groundfish fisheries: opportunities for reducing incidental catch of depleted species. Canadian Journal of Fisheries and Aquatic Sciences 72:1835–1846.

Boggs, C. H., and R. Y. Ito. 1993. Hawaii's pelagic fisheries. Marine Fisheries Review 55:69–82.

Bradford, A. L., R. W. Baird, S. D. Mahaffy, A. M. Gorgone, D. J. McSweeney, T. Cullins, D. L. Webster, and A. N. Zerbini. 2018. Abundance estimates for management of endangered false killer whales in the main Hawaiian Islands. Endangered Species Research 36:297–313.

Bradford, A. L., E. A. Becker, E. M. Oleson, K. A. Forney, J. E. Moore, and J. Barlow. 2020. Abundance estimates of false killer whales in Hawaiian waters and the broader Central Pacific. Pages 78. U.S. Department of Commerce, NOAA technical memorandum NOAA-TM-NMFS-PIFSC-104, Honolulu, Hawaii, USA.

Bradford, A. L., K. A. Forney, E. M. Oleson, and J. Barlow. 2014. Accounting for Subgroup Structure in Line-Transect Abundance Estimates of False Killer Whales (*Pseudorca crassidens*) in Hawaiian Waters. PLOS ONE 9:e90464.

Bradford, A. L., E. M. Oleson, R. W. Baird, C. H. Boggs, K. A. Forney, and N. C. Young. 2015. Revised stock boundaries for false killer whales (*Pseudorca crassidens*) in Hawaiian waters. Pages 29. U.S. Department of Commerce, NOAA Technical Memorandum NOAA-TM-NMFS-PIFSC-47, Honolulu, Hawaii, USA.

Carretta, J., K. Forney, M. Lowry, J. Barlow, J. Baker, D. Johnston, B. Hanson, M. Muto, D. Lynch, and L. Carswell. 2009. US Pacific marine mammal stock assessments: 2008. Pages 335. U.S. Department of Commerce, NOAA technical memorandum NOAA-TM-NMFS-SWFSC-434, La Jolla, California, USA.

Cayula, J.-F., and P. Cornillon. 1992. Edge detection algorithm for SST images. Journal of Atmospheric and Oceanic Technology 9:67–80.

Chelton, D. B., M. G. Schlax, and R. M. Samelson. 2011. Global observations of nonlinear mesoscale eddies. Progress in Oceanography 91:167–216.

Dunn, D. C., A. M. Boustany, J. J. Roberts, E. Brazer, M. Sanderson, B. Gardner, and P. N. Halpin. 2014. Empirical move-on rules to inform fishing strategies: a New England case study. Fish and Fisheries 15:359–375.

Esteban, R., P. Verborgh, P. Gauffier, J. Giménez, C. Guinet, and R. De Stephanis. 2016. Dynamics of killer whale, bluefin tuna and human fisheries in the Strait of Gibraltar. Biological Conservation 194:31–38.

Federal Register. 2012. Taking of marine mammals incidental to commercial fishing operations; False killer whale take reduction plan federal register 77 FR 71260. Pages 71260–71286. Federal Register, Washington, D.C., USA.

Fish, F. E. 1998. Comparative kinematics and hydrodynamics of odontocete cetaceans: morphological and ecological correlates with swimming performance. Journal of Experimental Biology 201:2867–2877.

Forney, K. A., E. A. Becker, D. G. Foley, J. Barlow, and E. M. Oleson. 2015. Habitat-based models of cetacean density and distribution in the central North Pacific. Endangered Species Research 27:1–20.

Forney, K., and D. Kobayashi. 2007. Updated Estimates of Mortality and Injury of Cetaceans in the Hawaii-based Longline Fishery, 1994-2005. U.S. Department of Commerce, NOAA Technical Memorandum NOAA-TM-NMFS-SWFSC-412, Santa Cruz, California, USA.

Forney, K. A., D. R. Kobayashi, D. W. Johnston, J. A. Marchetti, and M. G. Marsik. 2011. What's the catch? Patterns of cetacean bycatch and depredation in Hawaii-based pelagic longline fisheries. Marine Ecology 32:380–391.

Gardner, B., P. J. Sullivan, S. J. Morreale, and S. P. Epperly. 2008. Spatial and temporal statistical analysis of bycatch data: patterns of sea turtle bycatch in the North Atlantic. Canadian Journal of Fisheries and Aquatic Sciences 65:2461–2470.

Gilman, E. L., P. Dalzell, and S. Martin. 2006. Fleet communication to abate fisheries bycatch. Marine Policy 30:360–366.

Gilman, E., D. R. Kobayashi, and M. Chaloupka. 2008. Reducing seabird bycatch in the Hawaii longline tuna fishery. Endangered Species Research 5:309–323.

Gilman, E., D. Kobayashi, T. Swenarton, N. Brothers, P. Dalzell, and I. Kinan-Kelly. 2007. Reducing sea turtle interactions in the Hawaii-based longline swordfish fishery. Biological Conservation 139:19–28.

Hamer, D. J., S. J. Childerhouse, and N. J. Gales. 2012. Odontocete bycatch and depredation in longline fisheries: a review of available literature and of potential solutions. Marine Mammal Science 28: E345–E374.

Hamilton, S., and G. B. Baker. 2019. Technical mitigation to reduce marine mammal bycatch and entanglement in commercial fishing gear: lessons learnt and future directions. Reviews in Fish Biology and Fisheries 29:223–247.

Hazen, E. L., et al. 2017. WhaleWatch: a dynamic management tool for predicting blue whale density in the California Current. Journal of Applied Ecology 54:1415–1428.

Howell, E. A., D. R. Kobayashi, D. M. Parker, G. H. Balazs, and J. J. Polovina. 2008. TurtleWatch: a tool to aid in the bycatch reduction of loggerhead turtles *Caretta caretta* in the Hawaii-based pelagic longline fishery. Endangered Species Research 5:267–278.

Janc, A., G. Richard, C. Guinet, J. P. Y. Arnould, M. C. Villanueva, G. Duhamel, N. Gasco, and P. Tixier. 2018. How do fishing practices influence sperm whale (*Physeter macrocephalus*) depredation on demersal longline fisheries? Fisheries Research 206:14–26.

Jonsen, I., and T. Patterson. 2019. foieGras. Fit Continuous-Time State-Space and Latent Variable Models for Filtering Argos Satellite (and Other) Telemetry Data and Estimating Movement Behaviour. R Package Version 0.6-9. https://cran.r-project.org/package=foieGras

JPL MUR MEaSUREs Project. 2015. GHRSST Level 4 MUR Global Foundation Sea Surface Temperature Analysis. Ver. 4.1. NASA PO.DAAC, California, USA.

Lehodey, P., M. Bertignac, J. Hampton, A. Lewis, and J. Picaut. 1997. El Niño Southern Oscillation and tuna in the western Pacific. Nature 389:715–718.

Lindsay, R. E., R. Constantine, J. Robbins, D. K. Mattila, A. Tagarino, and T. E. Dennis. 2016. Characterising essential breeding habitat for whales informs the development of large-scale Marine Protected Areas in the South Pacific. Marine Ecology Progress Series 548:263–275.

Loosmore, N. B., and E. D. Ford. 2006. Statistical inference using the G or K point pattern spatial statistics. Ecology 87:1925–1931.

Martien, K. K., B. L. Taylor, S. J. Chivers, S. D. Mahaffy, A. M. Gorgone, and R. W. Baird. 2019. Fidelity to natal social groups and mating within and between social groups in an endangered false killer whale population. Endangered Species Research 40:219–230.

McCracken, M. L. 2010. Adjustments to false killer whale and short-finned pilot whale bycatch estimates. PIFSC Working Paper WP-10-007.

Mooney, T. A., A. Pacini, and P. E. Nachtigall. 2009. False killer whale (*Pseudorca crassidens*) echolocation and acoustic disruption: implications for longline bycatch and depredation. Canadian Journal of Zoology 87:726–733.

Mul, E., M. A. Blanchet, B. T. McClintock, W. J. Grecian, M. Biuw, and A. Rikardsen. 2020. Killer whales are attracted to herring fishing vessels. Marine Ecology Progress Series 652:1–13.

OBPG. 2014. Sea-viewing Wide Field-of-view Sensor (SeaWiFS) Ocean Color Data, NASA OB.DAAC Ocean Biology Processing Group (OBPG). Maintained by NASA Ocean Biology Distibuted Active Archive Center (OB.DAAC), Goddard Space Flight Center, Greenbelt, Maryland, USA.

Oleson, E. M., C. H. Boggs, K. A. Forney, M. B. Hanson, D. R. Kobayashi, B. L. Taylor, P. R. Wade, and

G. M. Ylitalo. 2010. Status review of Hawaiian insular false killer whales (*Pseudorca crassidens*) under the Endangered Species Act. Pages 140 + appendices. U.S. Department of Commerce, NOAA technical memorandum NOAA-TM-NMFS-PIFSC-22, Honolulu, Hawaii, USA.

R Core Team. 2018. R: A Language and Environment for Statistical Computing. R Foundation for Statistical Computing, Vienna, Austria. https://www.R-project.org/

Rabearisoa, N., P. Bach, P. Tixier, and C. Guinet. 2012. Pelagic longline fishing trials to shape a mitigation device of the depredation by toothed whales. Journal of Experimental Marine Biology and Ecology 433:55–63.

Rabearisoa, N., P. S. Sabarros, E. V. Romanov, V. Lucas, and P. Bach. 2018. Toothed whale and shark depredation indicators: a case study from the Reunion Island and Seychelles pelagic longline fisheries. PLOS ONE 13:e0202037.

Read, A. J. 2008. The looming crisis: interactions between marine mammals and fisheries. Journal of Mammalogy 89:541–548.

Richard, G., J. Bonnel, P. Tixier, J. P. Y. Arnould, A. Janc, and C. Guinet. 2020. Evidence of deep-sea interactions between toothed whales and longlines. Ambio 49:173–186.

Richard, G., F. Samaran, C. Guinet, and J. Bonnel. 2021. Settings of demersal longlines reveal acoustic cues that can inform toothed whales where and when to depredate. JASA Express Letters 1. 16004.

Ripley, B. D. 1977. Modelling spatial patterns. Journal of the Royal Statistical Society: Series B (Methodological) 39:172–212.

Roberts, J. J., B. D. Best, D. C. Dunn, E. A. Treml, and P. N. Halpin. 2010. Marine Geospatial Ecology Tools: an integrated framework for ecological geoprocessing with ArcGIS, Python, R, MATLAB, and C++. Environmental Modelling & Software 25:1197–1207.

Secchi, E. R., and T. Vaske. 1998. Killer whale (*Orcinus orca*) sightings and depredation on tuna and swordfish longline catches in southern Brazil. Aquatic Mammals 24:117–122.

Stenseth, N. C., A. Mysterud, G. Ottersen, J. W. Hurrell, K.-S. Chan, and M. Lima. 2002. Ecological effects of climate fluctuations. Science 297:1292–1296.

Stepanuk, J. E. F., A. J. Read, R. W. Baird, D. L. Webster, and L. H. Thorne. 2018. Spatiotemporal patterns of overlap between short-finned pilot whales and the U.S. pelagic longline fishery in the Mid-Atlantic Bight: an assessment to inform the management of fisheries bycatch. Fisheries Research 208:309–320.

TEC, I. 2009. Cetacean depredation in the Hawaii longline fishery: interviews of longline vessel owners and captains. Report prepared for National Oceanic and Atmospheric Administration National Marine Fisheries Service, Pacific Islands Regional Office, Honolulu, Hawaii, USA.

Thode, A., et al. 2015. Cues, creaks, and decoys: using passive acoustic monitoring as a tool for studying sperm whale depredation. ICES Journal of Marine Science 72:1621–1636.

Thode, A., J. Straley, C. O. Tiemann, K. Folkert, and V. O'Connell. 2007. Observations of potential acoustic cues that attract sperm whales to longline fishing in the Gulf of Alaska. The Journal of the Acoustical Society of America 122:1265–1277.

Thode, A., L. Wild, J. Straley, D. Barnes, A. Bayless, V. O'Connell, E. Oleson, and J. Sarkay. 2016. Using line acceleration to measure false killer whale (*Pseudorca crassidens*) click and whistle source levels during pelagic longline depredation. Journal of the Acoustical Society of America 140:3941–3951.

Thorne, L. H., R. W. Baird, D. L. Webster, J. E. Stepanuk, and A. J. Read. 2019. Predicting fisheries bycatch: A case study and field test for pilot whales in a pelagic longline fishery. Diversity and Distributions 25:909–923.

Thorne, L. H., H. J. Foley, R. W. Baird, D. l. Webster, Z. T. Swaim, and A. J. Read. 2017. Movement and foraging behavior of short-finned pilot whales in the Mid-Atlantic Bight: importance of bathymetric features and implications for management. Marine Ecology Progress Series 584:245–257.

Tixier, P., et al. 2019. Commercial fishing patterns influence odontocete whale-longline interactions in the Southern Ocean. Scientific Reports 9:1–11.

Tixier, P., et al. 2020. Assessing the impact of toothed whale depredation on socio-ecosystems and fishery management in wide-ranging subantarctic fisheries. Reviews in Fish Biology and Fisheries 30:203–217.

Tixier, P., N. Gasco, G. Duhamel, and C. Guinet. 2015*a*. Habituation to an acoustic harassment device (AHD) by killer whales depredating demersal longlines. ICES Journal of Marine Science 72:1673–1681.

Tixier, P., J. Vacquie Garcia, N. Gasco, G. Duhamel, and C. Guinet. 2015*b*. Mitigating killer whale depredation on demersal longline fisheries by changing fishing practices. ICES Journal of Marine Science 72:1610–1620.

Towers, J. R., P. Tixier, K. A. Ross, J. Bennett, J. P. Y. Arnould, R. L. Pitman, and J. W. Durban. 2019. Movements and dive behaviour of a toothfish-depredating killer and sperm whale. ICES Journal of Marine Science 76:298–311.

Werner, T. B., S. Northridge, K. M. Press, and N. Young. 2015. Mitigating bycatch and depredation

of marine mammals in longline fisheries. ICES Journal of Marine Science 72:1576–1586.

Wood, S. 2006. Generalized additive models: an introduction with R. First edition. CRC Press, Boca Raton, Florida, USA.

Wood, S. 2007. The mgcv package. R Package Version 2.8-33. https://cran.r-project.org/web/packages/mgcv/index.html

Wood, S. N. 2017. Generalized additive models: an introduction with R. Second edition. CRC Press, Boca Raton, Florida, USA.

Woodworth, P. A., G. S. Schorr, R. W. Baird, D. L. Webster, D. J. McSweeney, M. B. Hanson, R. D. Andrews, and J. J. Polovina. 2011. Eddies as offshore foraging grounds for melon-headed whales (*Peponocephala electra*). Marine Mammal Science 28:638–647.

Woodworth-Jefcoats, P. A., J. J. Polovina, and J. C. Drazen. 2018. Synergy among oceanographic variability, fishery expansion, and longline catch composition in the central North Pacific Ocean. Fishery Bulletin 116:228–239.

Zuur, A., E. N. Ieno, N. Walker, A. A. Saveliev, and G. M. Smith. 2009. Mixed effects models and extensions in ecology with R. Springer Science & Business Media, Berlin, Germany.

Supporting Information

Additional Supporting Information may be found online at: http://onlinelibrary.wiley.com/doi/10.1002/ecs2.3682/full